ELSEVIER

Ceramics International 30 (2004) 807–812

CERAMICS INTERNATIONAL

www.elsevier.com/locate/ceramint

Effects of alumina additions on sintering behavior of gadolinia-doped ceria

Joo-Sin Lee [a,*], Kwang-Hoon Choi [a], Bong-Ki Ryu [b], Byoung-Chul Shin [c], Il-Soo Kim [c]

[a] *Department of Materials Science and Engineering, Kyungsung University, Busan 608-736, South Korea*
[b] *School of Materials Science and Engineering, Pusan National University, Busan 609-735, South Korea*
[c] *Department of Information Materials Engineering, Dongeui University, Busan 614-714, South Korea*

Received 18 March 2003; received in revised form 26 May 2003; accepted 25 July 2003

Available online 19 March 2004

Abstract

The effects of alumina additions on the sintering behavior of gadolinia-doped ceria were systematically investigated in terms of the variations in sintered density and grain size and the existing forms of Al_2O_3 in CeO_2. Sintered density increased with increasing Al_2O_3 content up to 2 mol% and then it decreased with further addition of Al_2O_3. Grain size also increased with increasing Al_2O_3 content up to 2 mol% and then decreased with further addition of Al_2O_3. Decrease in grain size was caused by a pinning effect of Al_2O_3 precipitated at grain boundaries. Lattice constant decreased with increasing Al_2O_3 content up to 2 mol%. This decrease is due to the substitution of smaller Al^{3+} ions for Ce^{4+} ions in the CeO_2 structure. According to the results obtained from SEM and XRD analyses, the solubility limit of Al_2O_3 in $Ce_{0.8}Gd_{0.2}O_{1.9}$ ceramics was found to be nearly 2 mol%. The addition of Al_2O_3 up to the solubility limit was found to promote the sintering properties of Gd_2O_3-doped CeO_2.

Keywords: A. Sintering; D. Alumina; Gadolinia-doped ceria; Solubility limit; Coprecipitation

1. Introduction

Oxygen ionic conductors have a wide variety of applications in the field of electrochemistry. They can be used as solid electrolyte membranes in oxygen sensors, fuel cells, and oxygen pumps. Among the oxygen ionic conductors, Y_2O_3-stabilized ZrO_2 (YSZ) has been the most extensively investigated and practically used. However, especially for solid oxide fuel cell (SOFC) applications, a considerable research effort was devoted to developing alternative solid electrolytes for YSZ, which should possess higher electrical conductivity than YSZ and be operable at lower temperatures around 800 °C.

Ceria electrolyte has received much attention as an alternative to YSZ [1]. However, ceria-based ceramics are difficult to be densified below 1600 °C [2]. This makes them difficult for manufacturing ceria-based electrolytes which can be used for SOFC system because ceria-based electrolytes and other components such as cathode and anode have to be cofired.

In order to lower the sintering temperature, other methods utilizing fine starting powders and additives as sintering aids should be exploited. The preparation of ultra fine ceria-based ceramic powders has been studied by many investigators [2–9]. In contrast, only a limited number of reports are available as to the densification of ceria-based ceramics with the addition of sintering additives [10–14].

Yoshida et al. [10] reported that sintering of samaria-doped ceria was significantly promoted by the addition of a small amount of gallia. They reported that the samples sintered at 1450 °C with the addition of 1% gallium had almost the same average grain size and electrical conductivity as the samples sintered at 1600 °C with no addition of Ga_2O_3 had.

It has been also reported that the transition metal oxide additives enhance densification. The effects of cobalt oxide additions on the sintering characteristics and electrical properties of $Ce_{0.8}Gd_{0.2}O_{2-x}$ ceramics were investigated by Kleinlogel and Gauckler [11,12]. They reported that the

* Corresponding author. Tel.: +82-51-620-4763; fax: +82-51-622-8452.
E-mail address: leejs@star.kyungsung.ac.kr (J.-S. Lee).

0272-8842/$30.00
doi:10.1016/j.ceramint.2003.07.018

addition of a small amount of Co_3O_4 strongly enhanced the densification kinetics without changing the electrochemical performance of $Ce_{0.8}Gd_{0.2}O_{2-x}$ ceramics. The densification was explained by a liquid-phase sintering mechanism.

Zhang et al. [13,14] investigated the effects of the transition metal oxide additives on the sintering characteristics of undoped CeO_2. They reported that the addition of a small amount of Fe_2O_3 or CoO strongly enhanced the densification rate and promoted the grain boundary mobility. As a result, these additives could lower the sintering temperature of CeO_2.

It should be noted that studies on the sintering additives used for ceria-based ceramics have been limited to Ga_2O_3, Co_3O_4, Fe_2O_3 and CoO additives. The starting powders used have been either commercially available powders or doped powders prepared by the conventional mixed-oxide method.

In this work, the effects of alumina additions on the sintering behavior of gadolinia-doped ceria were systematically studied. Mixtures of Gd_2O_3, CeO_2, and Al_2O_3 were prepared by the coprecipitation method. Emphasis is especially placed on the variations in sintered density and grain size and the existing forms of Al_2O_3 in CeO_2.

2. Experimental procedure

Fig. 1 shows a schematic flow diagram of experimental procedure. Powders of Gd_2O_3-doped CeO_2 with different concentrations of Al_2O_3 were prepared by the coprecipitation method. A mixed aqueous solution having a composition corresponding to $(Ce_{0.8}Gd_{0.2}O_{1.9})_{1-x}(Al_2O_3)_x$ ($x = 0$, 0.01, 0.02, 0.03, 0.05) was obtained by mixing different aqueous solutions prepared from $Ce(NO_3)_3{\cdot}6H_2O$ powder (Acros Organics, 99.5%), $Gd(NO_3)_3{\cdot}6H_2O$ powder (Aldrich Chemical Co., 99.9%), and $Al(NO_3)_3{\cdot}9H_2O$ powder (Acros Organics, ≥99%), respectively. The salt containing the cations was then coprecipitated by adding an aqueous solution prepared from $(NH_4)_2C_2O_4{\cdot}H_2O$ powder (Junsei Chemical Co., 99.5%) and NH_4OH (Junsei Chemical Co., NH_3 28–30%) into the mixed aqueous solution.

The precipitates were washed with distilled water three times to remove the salt anions, followed by washing with ethyl alcohol three times to lighten the agglomeration. The precipitates were cleaned and dispersed in an ultrasonic cleaner under vigorous stirring. They were then vacuum-filtered and dried.

Drying was performed at about 120 °C in a drying oven for 1 h. The dried powders were then calcined at 700 °C for

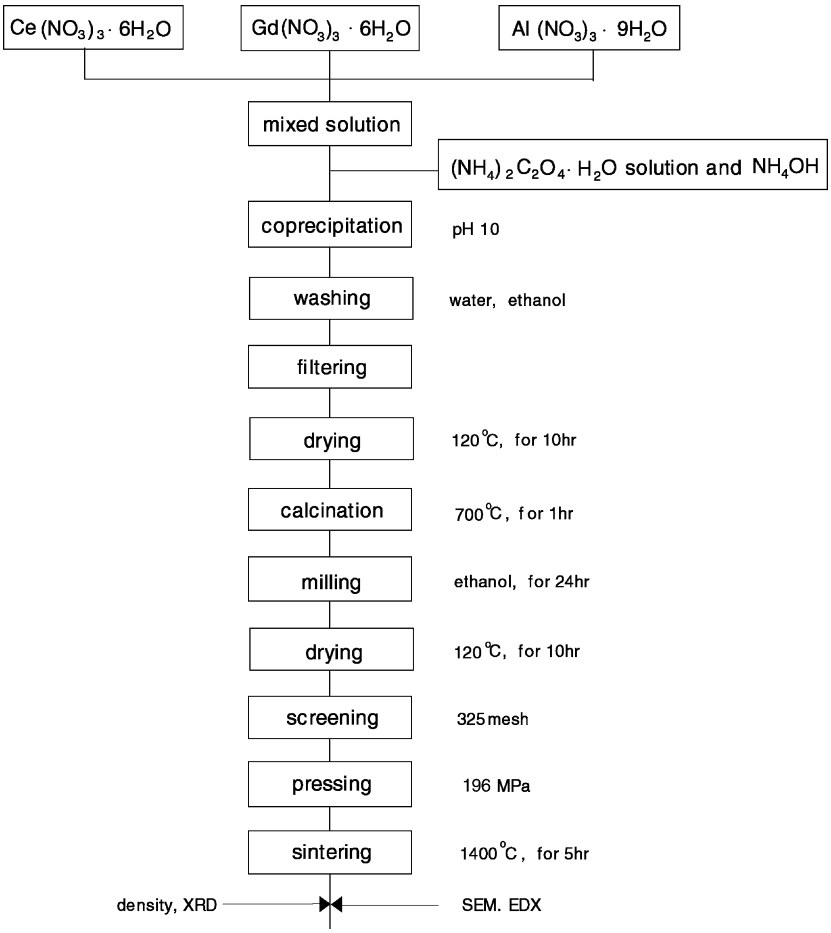

Fig. 1. Flowchart of experimental procedure.

1 h. To grind agglomerates produced during the calcination process, the calcined powders were ball-milled in ethanol for 24 h. For milling, a plastic jar and zirconia balls were used. After milling the calcined powders, the powders were dried again. After drying, the powders were screened to −325 mesh.

The sieved powders of −325 mesh size fraction were uniaxially dry-pressed at 196 MPa into pellets having a diameter of 12 mm and a thickness of 4 mm. The pellets were sintered at 1400 °C for 5 h. The heating rate was 10 °C/min.

The sintered densities were measured by using the Archimedes method with water and/or calculated from the weights and the dimensions of the specimens. It was found that both methods of obtaining the density provided almost the same value. An average value obtained from the five specimens was taken.

For microstructural investigation, the cross-section of the polished specimens was thermally etched. The specimens were then Au-coated and examined with a scanning electron microscope (SEM, Model S-2400 by Hitachi). The distribution of aluminum element was detected utilizing energy dispersive X-ray analysis spectroscopy (EDX, Model Sigma MS3 by Kevex).

X-ray diffraction (XRD) technique was employed to identify the phases present and to obtain the values of lattice constant. XRD was performed on the milled powders of specimens by using a Rigaku D/MAX IIIA diffractometer using Ni-filtered Cu Kα radiation.

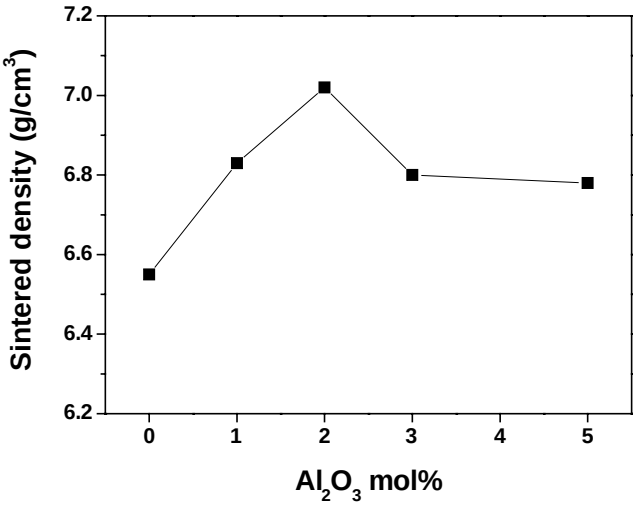

Fig. 2. Sintered density as a function of Al_2O_3 content.

3. Results and discussion

Fig. 2 shows the sintered density as a function of Al_2O_3 content. It is shown that the sintered density increases with

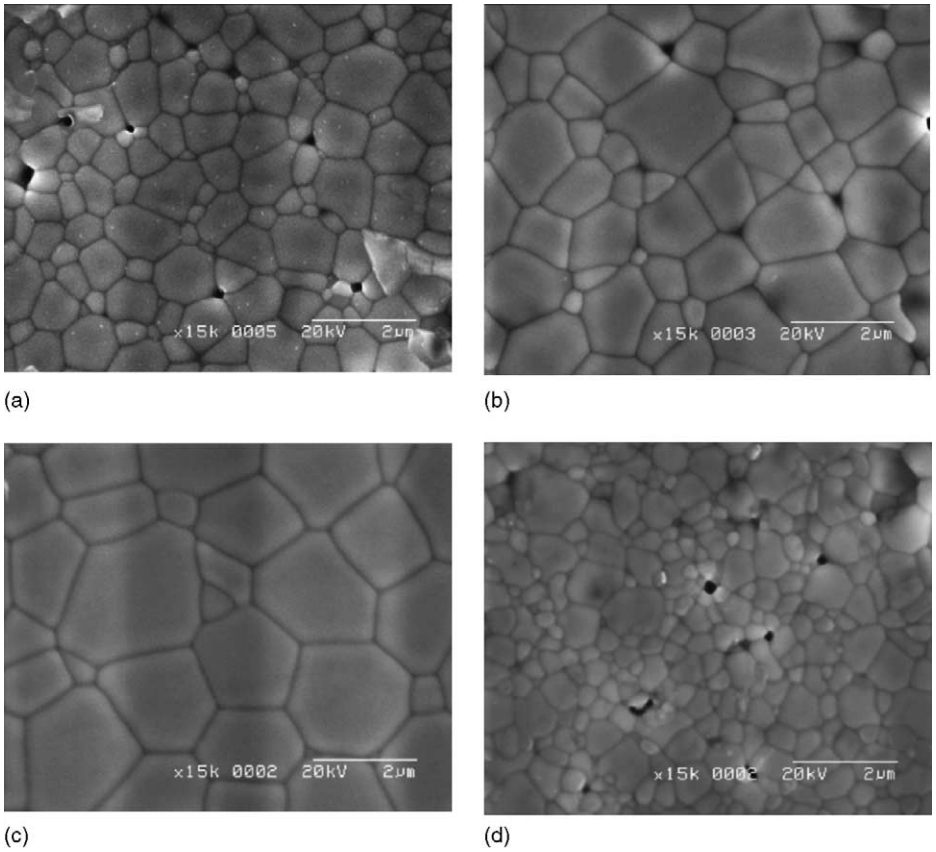

Fig. 3. SEM micrographs of the polished specimens with different Al_2O_3 contents. (a) 0 mol%, (b) 1 mol%, (c) 2 mol%, and (d) 5 mol%.

increasing Al_2O_3 content up to 2 mol%. The theoretical density of $Ce_{0.8}Gd_{0.2}O_{1.9}$ ceramics was calculated to be 7.279 g/cm^3 by applying the measured lattice parameter of 5.415 Å into the oxygen vacancy model. The sintered density of pure $Ce_{0.8}Gd_{0.2}O_{1.9}$ specimen was 90% of the theoretical density. The sintered density of the specimen containing 2 mol% Al_2O_3 was higher than that of pure specimen. The sintered density of the specimen containing 2 mol% Al_2O_3 was 96.4% of the theoretical density. With Al_2O_3 addition over 2 mol%, the sintered density decreased as shown in Fig. 2.

Fig. 3 shows the SEM micrographs of the polished specimens with different Al_2O_3 contents. The pure $Ce_{0.8}Gd_{0.2}O_{1.9}$ specimen had the average grain size of 1 μm or less while 1 mol% Al_2O_3-added specimen had larger average grain size. The increase in grain size was shown with Al_2O_3 addition up to 2 mol%. The grain size decreased and the precipitates appeared in grain boundaries with the addition of Al_2O_3 content above 3 mol%.

The precipitates were identified to be Al_2O_3 phase by EDX analysis. Fig. 4 shows a SEM micrograph and corresponding EDX spectra for the specimen containing 5 mol% Al_2O_3. The precipitates were spot-scanned for EDX analysis, and the result showed high Al concentration.

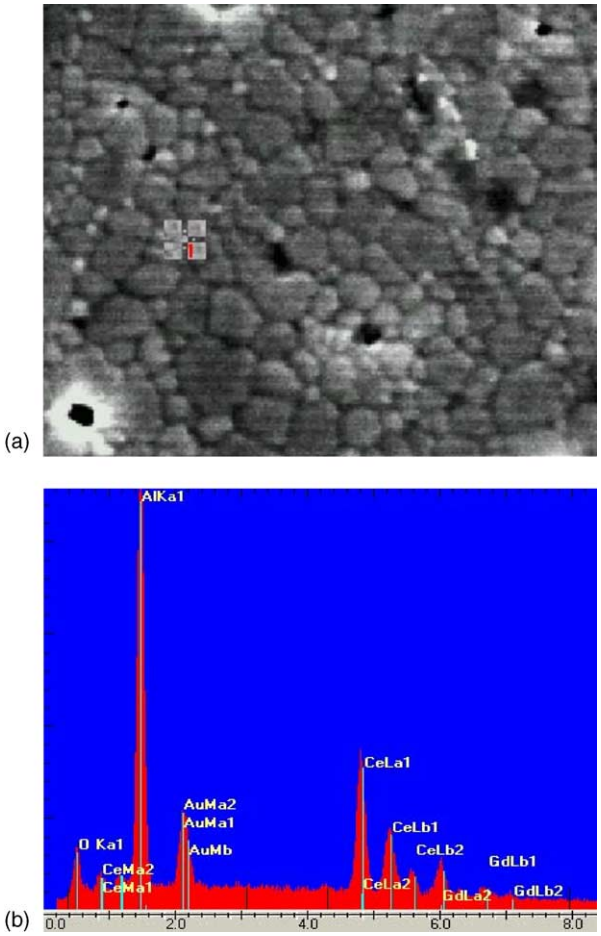

Fig. 4. (a) SEM micrograph and (b) corresponding EDX spectra for Gd_2O_3-doped CeO_2 containing 5 mol% Al_2O_3.

XRD pattern for 5 mol% Al_2O_3-added specimen is shown in Fig. 5. The peaks of cubic fluorite type mainly appeared. However, a series of peaks related with a new phase appeared also. The peaks of the new phase are marked as (◆) in Fig. 5. The new phase was identified as $AlGdO_3$.

To confirm the formation of $AlGdO_3$ at the same sintering condition used in this study, a mixed aqueous solution of $Al(NO_3)_3{\cdot}9H_2O$ and $Gd(NO_3)_3{\cdot}6H_2O$ was prepared. The coprecipitates obtained from this solution were calcined and sintered with the same conditions used in this study. XRD pattern of the sintered specimen is shown in a small window in Fig. 5. From this result, we could confirm that the $AlGdO_3$ formed at 1400 °C.

In the case of specimens with 0, 1, 2 and 3 mol% of Al_2O_3 addition, the peaks of cubic fluorite type were clearly shown in their XRD patterns, but the peaks of other phase were not detected probably because of the presence of a small amount.

The results of SEM and XRD analyses indicate that Al_2O_3 reacts with Gd_2O_3 to form $AlGdO_3$ phase and excess Al_2O_3 is precipitated.

Yoshida et al. [10] reported that gallium samarium garnet ($Ga_5Sm_3O_{12}$) phase was detected as a second phase in the case of samaria-doped ceria with ≥5% gallium addition. They reported XRD peaks of the second phase and a SEM image showing grains having a grain shape different from that of ceria in the case of 5% gallium-added specimen. They explained that the decrease in the average grain size was due to inhibition of grain growth by the second phase when the amount of gallium increased to ≥1%.

The XRD peaks for Gd_2O_3-doped CeO_2 specimens containing Al_2O_3 content up to 2 mol% were shifted to higher 2θ angles compared with those for pure Gd_2O_3-doped CeO_2. The peaks were shifted to higher angles as Al_2O_3 content increased. However, with Al_2O_3 additions over 2 mol% the peaks were not shifted further. Fig. 6 shows the lattice constant calculated from high-angle XRD patterns as a function of Al_2O_3 content.

The lattice constant decreased linearly with increasing Al_2O_3 content up to 2 mol%, but the value became almost constant when the content of Al_2O_3 was over 2 mol%. The decrease in lattice constant is apparently due to the substitution of smaller Al^{3+} ions (0.53 Å) [15] for Ce^{4+} ions (0.97 Å) [16] in the CeO_2 structure. Thus, the solid solubility limit of Al_2O_3 in Gd_2O_3-doped CeO_2 is estimated to be 2 mol%.

In general, dopants in alkaline earth oxide-doped ceria systems or rare earth oxide-doped ceria systems have large cation solubilities [16]. However, it is expected that a dissolution of Al_2O_3 in a CeO_2 system is limited because the ionic radius of Al^{3+} is much smaller than that of Ce^{4+}.

A high dissolution of dopants has been also shown in Y_2O_3-, CaO-, and MgO-doped ZrO_2 systems [17]. However, it has been reported that the equilibrium solubility of Al_2O_3

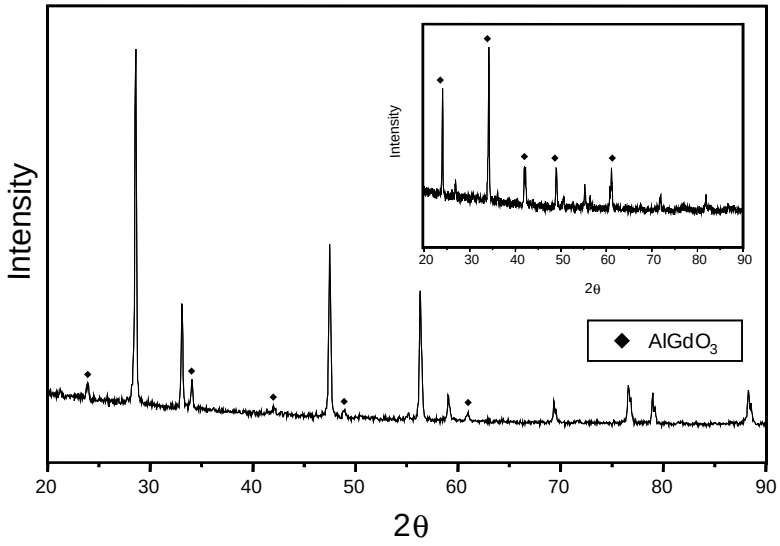

Fig. 5. X-ray diffraction pattern of Gd_2O_3-doped CeO_2 containing 5 mol% Al_2O_3.

in ZrO_2 was low because the ionic radius of Al^{3+} (0.53 Å) is much smaller than that of Zr^{4+} (0.84 Å) [15].

In the case of Al_2O_3 addition in Y_2O_3-stabilized ZrO_2, it has been reported that the estimated solubility limits of Al_2O_3 were 0.5 mol% at 1700 °C [18] and 0.1 mol% at 1300 °C [19]. It has been also reported that the equilibrium solubility of Al_2O_3 in CaO-stabilized ZrO_2 increased up to 1 mol% at 1400 °C by employing the coprecipitated powders [20].

In this study, the solid solubility limit of Al_2O_3 increased up to 2 mol% because the CeO_2 system could easily accommodate the additives due to its larger host lattice than ZrO_2 system and fine powders prepared by the coprecipitation method were homogeneously mixed at the atomic level.

As noted previously, it is possible that Al_2O_3 additions resulted in the substitution of Al^{3+} ions for Ce^{4+} ions within its solubility limit. Such substitution reaction can be described using Kroger–Vink notation which is given by

$$Al_2O_3 \xrightarrow{CeO_2} 2Al'_{Ce} + V_O^{\cdot\cdot} + 3O_O^{x} \quad (1)$$

The addition of Al_2O_3 in a CeO_2 system would lead to the formation of oxygen vacancies because of charge compensation. It is expected that these oxygen vacancies enhance the densification rate and promote the grain boundary mobility. Moreover, the addition of Al_2O_3 may induce the large distortion of the surrounding lattice because Al^{3+} ion has much smaller size compared with that of Ce^{4+} ion.

It is also expected that the lattice distortion promotes the grain boundary mobility due to the effect of severely undersized dopant [16]. In fact, in the case of Al_2O_3 addition in a CeO_2 system the increase in grain size with increasing Al_2O_3 content is much larger than that of Al_2O_3 addition in a ZrO_2 system [20]. A difference in ionic radius between the matrix Ce^{4+} ion (0.97 Å) and the additive Al^{3+} ion (0.53 Å) is larger than that between the matrix Zr^{4+} ion (0.84 Å) and the additive Al^{3+} ion (0.53 Å).

Both sintered density and grain size increased with increasing Al_2O_3 content up to 2 mol% and decreased with Al_2O_3 content above 3 mol%. These results indicate that Al_2O_3 additions within the solubility limit accelerate the densification rate remarkably and promote the grain boundary mobility.

However, at a higher Al_2O_3 content over the solubility limit, excess Al_2O_3 is precipitated. The precipitates inhibit the grain growth and lead to the decrease in grain size by a pinning effect. The precipitates cause the decline in density probably because the strain is produced due to the difference in both the elastic modulus and the thermal expansion coefficient between the precipitates (Al_2O_3) and CeO_2.

Al_2O_3 addition up to the solid solubility limit promoted the grain growth and densification. It is suggested that

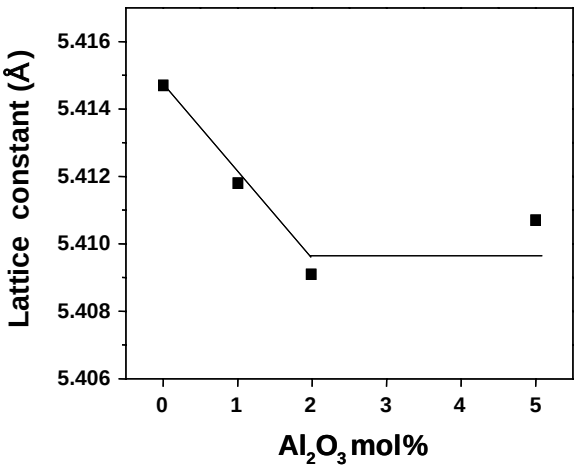

Fig. 6. Lattice constant as a function of Al_2O_3 content.

soluble Al_2O_3 has a beneficial effect on the sintering behavior of Gd_2O_3-doped CeO_2.

4. Conclusion

The effects of alumina additions on the sintering behavior of gadolinia-doped ceria were systematically investigated in terms of the variations in sintered density and grain size and the existing forms of Al_2O_3 in CeO_2.

The density of sintered Gd_2O_3-doped CeO_2 increased with increasing Al_2O_3 content up to 2 mol%. However, it decreased with further addition of Al_2O_3 above 3 mol%. Grain size also increased with increasing Al_2O_3 content up to 2 mol% but it decreased with further addition of Al_2O_3 in a way similar to the density. At higher Al_2O_3 content, grain size decreased by a pinning effect induced by Al_2O_3 precipitates appeared at grain boundaries. The solubility limit of Al_2O_3 in $Ce_{0.8}Gd_{0.2}O_{1.9}$ ceramics estimated using the results obtained from SEM and XRD analyses was about 2 mol%. The addition of Al_2O_3 up to the solid solubility limit caused the promotion of grain growth and an increase in density. It is suggested that soluble Al_2O_3 gives an affirmative effect on the sintering behavior of Gd_2O_3-doped CeO_2.

Acknowledgements

This work was supported by ECC (Electronic Ceramics Center) at Dong-eui University as RRC·TIC program which is financially supported by KOSEF (Korea Science and Engineering Foundation) under MOST (Ministry of Science and Technology), ITEP (Korea Institute of Industrial Technology Evaluation and Planning) under MOCIE (Ministry of Commerce, Industry and Energy), and Busan Metropolitan City.

References

[1] H. Inaba, H. Tagawa, Ceria-based solid electrolytes, Solid State Ionics 83 (1996) 1–6.
[2] J.V. Herle, T. Horita, T. Kawada, N. Sakai, H. Yokokawa, M. Dokiya, Fabrication and sintering of fine yttria-doped ceria powder, J. Am. Ceram. Soc. 80 (4) (1997) 933–940.
[3] A. Overs, I. Riess, Properties of the solid electrolyte gadolinia-doped ceria prepared by thermal decomposition of mixed cerium–gadolinium oxalate, J. Am. Ceram. Soc. 65 (12) (1982) 606–609.
[4] P.L. Chen, I.W. Chen, Reactive cerium (IV) oxide powders by the homogeneous precipitation method, J. Am. Ceram. Soc. 76 (6) (1993) 1577–1583.
[5] Y.C. Zhou, M.N. Rahaman, Hydrothermal synthesis and sintering of ultrafine CeO_2 powders, J. Mater. Res. 8 (7) (1993) 1689–1696.
[6] K. Yamashita, K.V. Ramanujachary, M. Greenblatt, Hydrothermal synthesis and low temperature conduction properties of substituted ceria ceramics, Solid State Ionics 81 (1995) 53–60.
[7] A.K. Bhattacharya, A. Hartridge, K.K. Mallick, J.L. Woodhard, Low-temperature synthesis and characterization of ceria-based oxide ion conductors, J. Mater. Sci. 31 (1996) 5005–5007.
[8] J.V. Herle, T. Horita, T. Kawada, N. Sakai, H. Yokokawa, M. Dokiya, Low temperature fabrication of (Y, Gd, Sm)-doped ceria electrolyte, Solid State Ionics 86–88 (1996) 1255–1258.
[9] K. Higashi, K. Sonoda, H. Ono, S. Sameshima, Y. Hirata, Synthesis and sintering of rare-earth-doped ceria powder by the oxalate coprecipitation method, J. Mater. Res. 14 (3) (1996) 957–967.
[10] H. Yoshida, K. Miura, J. Fujita, T. Inagaki, Effect of gallia addition on the sintering behavior of samaria-doped ceria, J. Am. Ceram. Soc. 82 (1) (1999) 219–221.
[11] C.M. Kleinlogel, L.J. Gauckler, Sintering and properties of nanosized ceria solid solutions, Solid State Ionics 135 (2000) 567–573.
[12] C.M. Kleinlogel, L.J. Gauckler, Mixed electronic-ionic conductivity of cobalt doped cerium gadolinium oxide, J. Electroceram. 5 (3) (2000) 231–243.
[13] T. Zhang, P. Hing, H. Huang, J. Kilner, Densification, microstructure and grain growth in the CeO_2–Fe_2O_3 system ($0 \leq Fe/Ce \leq 20\%$), J. Eur. Ceram. Soc. 21 (2001) 2221–2228.
[14] T. Zhang, P. Hing, H. Huang, J. Kilner, Sintering and grain growth of CoO-doped CeO_2 ceramics, J. Eur. Ceram. Soc. 22 (2002) 27–34.
[15] R.D. Shannon, C.T. Prewitt, Effective ionic radii in oxides and fluorides, Acta Cryst. B25 (5) (1969) 925–946.
[16] P.L. Chen, I.W. Chen, Grain growth in CeO_2: dopant effects, defect mechanism, and solute drag, J. Am. Ceram. Soc. 79 (7) (1996) 1793–1800.
[17] T.H. Etsell, S.N. Flengas, Electrical properties of solid oxide electrolytes, Chem. Rev. 70 (3) (1970) 339–376.
[18] M. Miyayama, H. Yanagida, A. Asada, Effects of Al_2O_3 additions on resistivity and microstructure of yttria-stabilized zirconia, Am. Ceram. Soc. Bull. 65 (4) (1986) 660–664.
[19] M.J. Verkerk, A.J.A. Winnubst, A.J. Burggraaf, Effect of impurities on sintering and conductivity of yttria-stabilized zirconia, J. Mater. Sci. 17 (1982) 3113–3122.
[20] Y.G. Choi, J.S. Lee, H.D. Kim, Effects of Al_2O_3 additions on microstructure and conductivity of CaO-stabilized ZrO_2, Korean J. Mater. Res. 8 (3) (1998) 256–262.